Advances in Science and Technology Research Journal

Advances in Science and Technology Research Journal, 2026, 20(10), 391–406
https://doi.org/10.12913/22998624/225677
ISSN 2299-8624, License CC-BY 4.0

Received: 2026.06.25
Accepted: 2026.07.28
Published: 2026.09.01

Machine learning-assisted static stability region classification and magnetomotive force prediction for design-stage evaluation of a lifting electromagnet in suspension mode

Areg Grigoryan[1], Armine Avetisyan[1*], Arsen Hovhannisyan[1]

[1] Automation and Electromagnetic Systems Research Laboratory, National Polytechnic University of Armenia, Armenia

* Corresponding author's e-mail: arm.avetisyan@seua.am

ABSTRACT

Lifting electromagnets are widely used for attracting, holding, and transporting ferromagnetic loads. In addition to contact-based operation, in which the load is brought into direct contact with the electromagnet poles, such systems can also function as electromagnetic suspension devices, where the load is maintained at a specified air gap without mechanical contact with the poles. In this case, static admissible operation is defined by the balance between the load weight and the electromagnetic attractive force within allowable air-gap and force limits. This study proposes a machine learning-assisted framework for static stability-region classification and magnetomotive force prediction in the design-stage evaluation of a lifting electromagnet operating in suspension mode. A computational database was generated from the mathematical model of the electromagnet, where the air gap g, magnetomotive force F, and electromagnetic attractive force were considered as the main design variables. The database contained 13992 calculated operating points, with g varying from 4.8×10^{-5} to 3.1605×10^{-3} m, P_E from 0.22301 to 341.715326 N, and F from 150 to 425 A·turns. The predefined static stability-region limits resulted in 448 stable and 13,544 unstable samples. Random Forest, Gradient Boosting, and Decision Tree classifiers were trained and compared using the area under the receiver operating characteristic curve (AUC) as the main metric. The Decision Tree Classifier achieved the best result for the considered dataset, with an AUC of 1.000 and the shortest training and prediction times. A regression problem was then formulated to predict the required magnetomotive force for specified air-gap and electromagnetic-force values. Random Forest, Gradient Boosting, multilayer perceptron, and CatBoost regressors were evaluated. The CatBoost Regressor achieved the highest overall prediction accuracy, with a coefficient of determination R^2=0.999, root mean square error of 1.7933 A·turns, mean absolute error of 1.2746 A·turns, mean absolute percentage error of 0.4630%, and a prediction time of approximately 0.000023 s. The obtained results show that the proposed framework can serve as a design-stage surrogate tool for rapid static operating-region classification and magnetomotive force prediction.

Keywords: lifting electromagnet, electromagnetic suspension, machine learning, classification, regression, stability region, magnetomotive force.

INTRODUCTION

Lifting electromagnets are widely used in industrial systems for attracting, holding, and transporting ferromagnetic loads. Their operation is based on the generation of an electromagnetic attractive force that must be sufficient to overcome the weight of the load and ensure reliable interaction between the load and the poles of the electromagnet. In conventional applications, the attracted body is brought into contact with the poles. However, in some electromechanical systems, a lifting electromagnet can also operate as an electromagnetic suspension device, where the load is maintained at a prescribed distance from the poles without mechanical contact. In this case, the air gap between the load and the poles becomes one of the key parameters determining the operating state of the system.

The design of a lifting electromagnet operating in suspended mode is similar to that of a contact-type electromagnet. However, in this case, the key requirement is not only to generate sufficient attractive force but also to maintain a stable balance between the load's weight and the electromagnetic attractive force. For a given gravitational force of the load P_L, the electromagnet must provide the corresponding electromagnetic attractive force P_E at a prescribed air gap g. Consequently, the stability condition can be expressed as a balance between the load's gravitational force and the electromagnetic attractive force. In practical electromagnetic suspension design, this condition for the device must be ensured not only at a single operating point, but also within a specified stability region, defined by permissible variations in the air gap and attractive force.

The stability region of a lifting electromagnet can be defined by the permissible limits of variation of the air gap size and the electromagnetic attractive force. If the air gap varies between g_{min} and g_{max}, and the attractive force varies between P_E^{min} and P_E^{max}, the electromagnet must be capable of producing the required force values throughout this region. This requirement leads to two important design questions. The first question is whether the considered electromagnet configuration can provide the necessary combinations of g, P_E, and magnetomotive force F, ($F=Iw$, where I is the coil DC current and w is number of turns) for all points of the stability region. The second question is whether the electromagnet design under consideration can obtain the required magnetomotive force without violating the permissible thermal state of the control coil. Thus, the design process includes tasks associated with the need to take into account and comply with both electromagnetic and thermal constraints.

Classical design approaches for lifting and related electromagnets are usually based on magnetic equivalent circuits, analytical or numerical force calculations, parametric analysis, and finite element simulations [1–4]. These approaches provide physically interpretable results and make it possible to evaluate the electromagnetic force, magnetic flux distribution, air-gap behavior, and control winding parameters. However, when a large number of design variants and operating points must be analyzed, repeated solution of the mathematical model becomes computationally demanding. This limitation is especially important when the designer needs to evaluate the behavior of the electromagnet over an entire stability region rather than at a single nominal operating point.

Machine learning (ML) and data-driven models have been increasingly used for the design, analysis, surrogate modeling, and optimization of electromagnetic devices. Li et al. reviewed recent developments in ML-based design optimization of electromagnetic devices and showed that artificial neural networks, support vector machines, Gaussian-process-based models, random forests, and deep learning methods can be effectively used to approximate computationally expensive electromagnetic simulations and accelerate design procedures [5]. Lowther discussed the broader role of artificial intelligence and machine learning in the design and analysis of electromagnetic devices, emphasizing their potential for reducing computational effort in engineering design tasks [6]. More recently, Li et al. presented a review of data-driven models for electromagnetic device design and analysis, highlighting their applicability to prediction, optimization, and surrogate modeling problems [7]. Cheng et al. specifically analyzed data-driven surrogate models for electric motor design optimization, showing how such models can reduce the number of expensive numerical simulations required during iterative design [8]. In addition, Orosz et al. discussed robust design optimization and emerging technologies for electrical machines, emphasizing the need for efficient computational approaches in modern electromagnetic device design [9].

Surrogate models have also been applied to predict specific electromagnetic quantities and objective functions. Tahkola et al. used artificial neural networks for surrogate modeling of electrical machine torque, demonstrating the applicability of data-driven models to electromagnetic performance prediction [10]. Tucci et al. proposed a regularized deep learning procedure for topology optimization of electromagnetic devices, showing the potential of deep learning in complex electromagnetic design problems [11]. Lei et al. developed radial basis function models and sequential optimization strategies for electromagnetic device design, demonstrating the usefulness of surrogate-assisted optimization in reducing computational cost [12]. Similar machine learning-assisted approaches have also been developed in antenna and broader electromagnetics applications, where ML and deep learning methods have been used for antenna design, optimization, and selection [13].

In the authors' previous studies, related machine learning-assisted and hybrid heuristic–machine learning approaches were applied to electromagnet material and operational cost optimization [14], magnetorheological brake performance improvement [15], optimal design and parameter optimization of electromagnetic systems [16], [17], and automated modeling of electromagnetic systems with magnetorheological fluid [18]. These studies provide a methodological basis for using machine learning not only as a prediction tool, but also as a design-stage decision-support instrument for electromagnetic systems.

For electromagnetic suspension systems, the stability problem is primarily associated with maintaining the air gap within admissible limits while providing the required electromagnetic force. For this reason, a significant part of the existing literature focuses on air-gap control and dynamic stabilization of magnetic levitation in electromagnetic suspension systems. Zhang et al. proposed a model predictive control strategy for a magnetic levitation system using two-level state feedback. In their approach, measurable state variables, including the air gap, acceleration, and control current, were used to construct a prediction model and improve the transient response and disturbance resistance of the levitation system [19]. Similarly, Kim proposed a robust air-gap control method for a superconducting-hybrid MagLev intelligent conveyor system and demonstrated its applicability to stabilizing the air gap in a contactless conveyor system [20].

A related group of studies considers bounded air-gap constraints as a safety and stability requirement in Maglev systems. Xu et al. developed a robust levitation control approach for nonlinear uncertain Maglev systems with guaranteed bounded air gap, where the air-gap constraint was introduced to prevent undesirable contact between the suspended chassis and the guideway [21]. Later, Xu et al. proposed an adaptive robust constrained state control method for a nonlinear Maglev vehicle, also emphasizing the importance of maintaining the air gap within prescribed bounds under uncertainty and external disturbances [22]. Sun et al. further extended this direction by developing a deep learning-based semi-supervised control method for vertical security of a Maglev vehicle with guaranteed bounded air gap [23]. These studies demonstrate that air-gap limitation and stability are fundamental requirements in electromagnetic suspension systems. However, their main focus is dynamic control and safety assurance during operation, rather than design-stage classification of admissible operating regions.

Another important research direction is the use of surrogate models and machine learning methods for fast prediction of electromagnetic quantities. Feng et al. proposed a shallow neural network-based surrogate model for electromagnetic force calculation in Maglev vehicle dynamics simulation. Their model was designed to account for spatial relative position deviations and was validated against finite element simulation results, showing high agreement and practical applicability for dynamic simulation [24]. In the broader field of electrical machines, Tahkola et al. investigated surrogate modeling of electromagnetic torque using artificial neural networks trained on physics-based simulation data. Their study demonstrated that data-driven surrogate models can significantly improve computational efficiency while preserving acceptable accuracy in electromagnetic system analysis [10]. These works confirm the feasibility of replacing repeated computationally expensive simulations with trained prediction models when a representative database is available.

Data-driven and machine learning-based approaches have also been increasingly applied to the evaluation, monitoring, and optimization of Maglev and electromagnetic suspension systems. Zhou et al. proposed a data-driven comprehensive evaluation method for an electromagnetic suspension Maglev control system, combining improved evaluation indices with grey relational analysis to assess suspension gap stability and operation smoothness [25]. More generally, recent review studies show that machine learning is being actively used in Maglev transportation systems for modeling, control, optimization, gap prediction, fault diagnosis, and predictive maintenance [26]. These studies indicate a clear trend toward intelligent and data-driven analysis of electromagnetic suspension systems.

To better distinguish the proposed approach from previous studies, Table 1 compares representative works on Maglev and electromagnetic suspension systems in terms of the investigated system, applied method, main output, and difference from the present study.

Despite these advances, the combined use of classification and regression methods for the design-stage analysis of a lifting electromagnet operating in suspension mode remains insufficiently addressed. In contrast to the reviewed studies, the present work formulates the problem as a combined machine learning task: classification is used to determine whether calculated operating points belong to a predefined static stability region, while regression is used to predict the required magnetomotive force for specified values of the air gap and electromagnetic attractive force. Thus, the proposed approach transforms the mathematical model of the lifting electromagnet into a machine learning-assisted design-stage framework for rapid static stability-region assessment and magnetomotive force prediction.

The novelty of this study is the formulation of the lifting electromagnet design problem as a combined machine learning task in which a predefined static stability region is used for classification of admissible operating states, while regression models are used to predict the magnetomotive force required for suspension operation. This provides a data-driven surrogate framework for rapid design-stage assessment based on a mathematical model of the electromagnet

The main contributions of this study are summarized as follows:

1. A static stability-region-based classification formulation is proposed for a lifting electromagnet operating in suspension mode.
2. A computational database generated from the mathematical model of the electromagnet is used to construct a design-stage machine learning framework.
3. Classification models are used to rapidly identify admissible and inadmissible operating states according to predefined air-gap and electromagnetic-force limits.
4. Regression models are used to predict the magnetomotive force required for specified values of the air gap and electromagnetic attractive force.
5. The predicted magnetomotive force values provide input information for subsequent evaluation of control coil thermal feasibility and for integration into an automated design workflow.

MATERIALS AND METHODS

Lifting electromagnet and mathematical model

A lifting electromagnet operating in suspension mode must maintain a ferromagnetic load at a prescribed distance from its poles without direct mechanical contact. In this operating mode, the load is attracted by the electromagnetic force, but it does not touch the poles of the electromagnet. Instead, it remains suspended at a certain air gap g. Therefore, the air gap

Table 1. Comparison of related studies with the proposed approach

Study	System / object	Method	Main output	Difference from the present study
Zhang et al. [19]	Magnetic levitation system	Model predictive control	Air-gap control and disturbance resistance	Focused on dynamic control, whereas the present study addresses design-stage static stability-region classification and magnetomotive force prediction for a lifting electromagnet
Xu et al. [21],[22]	Maglev system	Robust/adaptive constrained control	Bounded air-gap control	Focused on constrained control under uncertainty, whereas the present study evaluates admissible operating states without solving a feedback-control problem
Sun et al. [23]	Maglev vehicle	Deep learning-based semi-supervised control	Vertical safety with bounded air gap	Focused on operational safety and control of Maglev vehicles, whereas the present study considers a lifting electromagnet in suspension mode
Feng et al. [24]	Maglev vehicle	Spiking neural network surrogate model	Electromagnetic force prediction	Predicts electromagnetic force for dynamic simulation, whereas the present study predicts the required magnetomotive force for specified g and P_E
Zhou et al. [25]	EMS Maglev control system	Data-driven evaluation	Suspension gap stability and operation smoothness evaluation	Evaluates control-system performance, whereas the present study uses machine learning for design-stage static stability-region classification and required F prediction

becomes one of the most important design and control parameters of the system. A schematic representation of the investigated lifting electromagnet operating in suspension mode is shown in Figure 1. The electromagnet consists of a magnetic base, core, cylinder, and control coil, which generates the magnetomotive force F. The ferromagnetic load is located below the pole surface and is separated from it by the air gap g. Under excitation of the control coil, the magnetic flux created in the magnetic circuit gives rise to the electromagnetic attractive force P_E, while the load is subjected to the gravitational force P_L. The objective of suspension operation is to maintain the load at the prescribed air gap by balancing these forces.

The mathematical model of the lifting electromagnet used in this study is based on the direct and inverse magnetic-circuit formulation and the electromagnetic force calculation procedure described in the authors' previous study [27]. The model is based on a nonlinear magnetic equivalent circuit (MEC) formulation for a lifting electromagnet and provides a unified computational framework for solving both direct and inverse magnetic-circuit problems. In this formulation, the electromagnet is represented by the ferromagnetic regions of the base, core, and cylindrical sections, the working air gap, the attracted load, and leakage magnetic flux paths. The model accounts for distributed magnetomotive force, nonlinear ferromagnetic reluctances, and leakage fluxes discretized into an arbitrary number of parallel branches, where the number of branches is selected according to the required solution accuracy. The nonlinear magnetic behavior of the ferromagnetic components is described using material magnetization curves; therefore, magnetic saturation is included in the calculation procedure. The resulting nonlinear algebraic system is solved using a Newton-based numerical algorithm with a sparse linear solver, which enables efficient computation even for a large number of leakage-flux branches. In [27], the model was experimentally validated using a prototype lifting electromagnet fabricated from AISI 1045 steel and tested on the Ani-1 experimental platform; the deviation between the calculated and measured lifting forces did not exceed 6.9%. Therefore, this model was used in the present study as a physically grounded and validated data-generation tool for constructing the machine learning database.

In the present study, the fixed structural parameters and material characteristics of the investigated electromagnet were kept unchanged. The main dimensions were r_1 = 10.45 mm, r_2 = 25.40 mm, r_3 = 27.55 mm, b_{ld} = 6.30 mm, b_{bs} = 7.30 mm, l_{cr} = 29.50 mm as shown in Figure 1(b). The air gap g, magnetomotive force F, and electromagnetic attractive force P_E were considered as the main variables for constructing the computational database. Each calculated operating point was represented by the triplet (g, F, P_E).

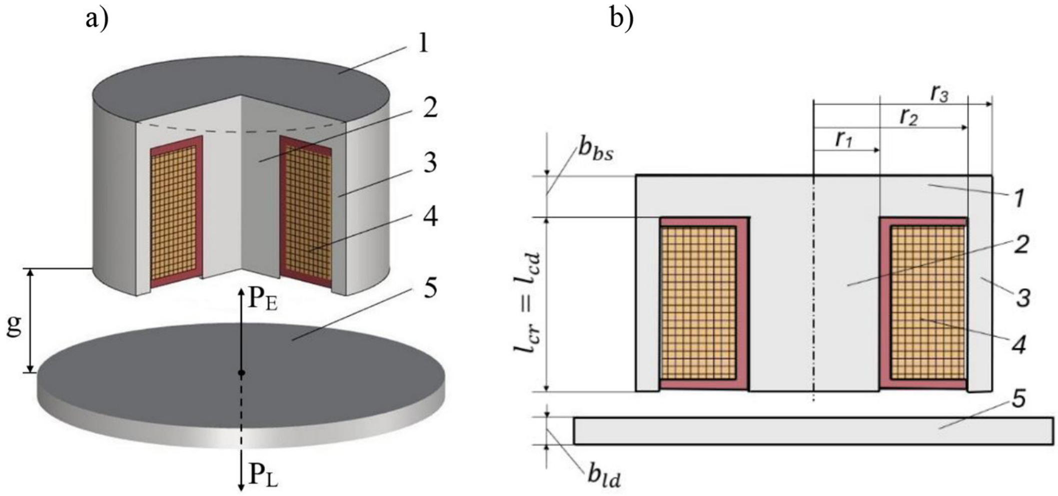

Figure 1. Schematic representation of the lifting electromagnet operating in suspension mode. 1 – ferromagnetic base, 2 – ferromagnetic core, 3 – ferromagnetic cylinder, 4 – control coil, 5 – ferromagnetic load g – air gap, – gravitational force of the load, – electromagnetic attractive force, l_{cr} – length of core and cylinder, b_{bs}, b_{ld} – thikness of base and load, r_1 – radius of the core, r_2, r_3 – inner and outer radii of the cylinder (adapted from [27])

The mathematical model presented in [27] was used here as the physical basis for data generation. Rather than repeatedly solving the model during design-stage analysis, the calculated data was organized into a computational database and subsequently used to train machine learning models for classification and prediction tasks.

Stability region formulation

For a lifting electromagnet operating as a suspension device, the basic stability condition is determined by the equilibrium between the load weight and the electromagnetic attractive force. This condition can be written as

$$P_L = P_E \quad (1)$$

where: P_L is the gravitational force of the load and P_E is the electromagnetic attractive force generated by the electromagnet.

In practical operation, exact equality between P_L and P_E at a single air-gap value is not sufficient for reliable suspension. The system must remain operational when the air gap and electromagnetic force vary within admissible limits. Therefore, a stability region is introduced, as illustrated in Figure 2. This region is bounded by the minimum and maximum allowable values of the air gap, g_{min} and g_{max}, and by the minimum and maximum allowable values of the electromagnetic attractive force, P_E^{min} and P_E^{max}.

Let g_0 be the prescribed nominal air gap, while g_{min} and g_{max} define the minimum and maximum allowable values of the air gap, respectively. Similarly, let P_E^{min} and P_E^{max} define the allowable range of the electromagnetic attractive force around the gravitational foce of the load P_L. Then the stability region can be expressed as

$$g_{\min} \leq g \leq g_{\max} \quad (2)$$

$$P_E^{min} \leq P_E \leq P_E^{max} \quad (3)$$

Thus, an operating point of the lifting electromagnet can be described by the pair (g' P_E). This point belongs to the stability region if both the air-gap condition and the electromagnetic-force condition are simultaneously satisfied. Otherwise, the point is considered to be outside the stability region.

For the considered design example, the following numerical values were used to define the static stability region:

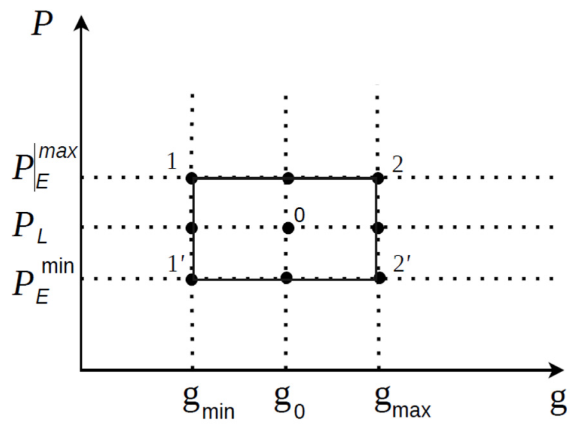

Figure 2. Graphical representation of the stability condition for maintaining the load at a prescribed air gap

$$g_0 = 0.00075\ m,$$
$$g_{\min} = 0.0005\ m, g_{\max} = 0.001\ m,$$
$$P_l = 10\ N,$$
$$P_E^{min} = 8\ N, P_E^{max} = 12\ N.$$

These values define a rectangular static stability region in the (g' P_E) plane. The main design requirement is that the lifting electromagnet must be able to provide the required electromagnetic attractive force for all characteristic points of this region by means of an appropriate value of the magnetomotive force *F*.

The selected numerical limits define a demonstration design case used to test the proposed classification–prediction framework. They are not intended to represent universal industrial limits. In practical design, the allowable air-gap and force limits should be selected according to the load requirements, allowable displacement tolerance, safety margins, and thermal and electromagnetic constraints of the specific application.

Based on the defined stability region, the first design problem is formulated as a binary classification problem. Each calculated operating point is assigned to one of two classes: stable or unstable. The target class variable *y* is defined as:

$$y = \begin{cases} 1, & \text{if } g_{\min} \leq g \leq g_{\max} \text{ and } P_E^{min} \leq P_E \leq P_E^{max} \\ 0, & \text{otherwise.} \end{cases} \quad (4)$$

Here, $y = 1$ denotes an operating point that belongs to the predefined stability region, whereas $y = 0$ denotes an operating point outside this region. Therefore, the classification model is trained to identify whether a given combination of air gap and electromagnetic attractive force satisfies stability requirements.

The second design problem is formulated as a regression-based prediction problem. In this case, the aim is to determine the magnetomotive force required to obtain a specified value of the electromagnetic attractive force at a given air gap. Therefore, the air-gap g and the electromagnetic attractive force P_E are considered as input variables, while the magnetomotive force F is considered as the target variable. The regression model approximates the following functional relationship:

$$F = f(g, P_E) \quad (5)$$

The predicted values of F are important not only for electromagnetic performance assessment, but also for assessing the performance of the electromagnet based on the thermal state of the control coil. If the required magnetomotive force leads to a control coil temperature exceeding the allowable limit, the corresponding electromagnet design must be revised. Thus, the proposed formulation combines stability-region classification with magnetomotive force prediction and provides a data-driven basis for further design verification.

In this way, the conventional mathematical model of the lifting electromagnet is transformed into a data-driven static stability assessment framework. In the proposed formulation, classification is used to identify admissible and inadmissible operating states with respect to the predefined stability region, while regression is used to predict the magnetomotive force required for suspension control. This combination enables rapid analysis of electromagnet operating conditions and reduces the need for repeated direct resource-intensive calculations during the design stage.

The formulated stability conditions define the basis for constructing the classification and prediction tasks. In the next section, the computational database generated from the mathematical model is described, and the machine learning methodology used for stability-region classification and magnetomotive force prediction is presented.

COMPUTATIONAL DATABASE AND MACHINE LEARNING METHODOLOGY

The proposed machine learning-based approach was implemented using a computational database generated from the mathematical model of the lifting electromagnet presented in [27]. The database contains calculated operating points corresponding to different values of the air gap, magnetomotive force, and electromagnetic attractive force. Each row of the database represents one calculated state of the electromagnet and includes the variables required for classification and prediction tasks.

The database contained 13992 calculated operating points, with g varying from 4.8×10^{-5} to 3.1605×10^{-3} m, P_E from 0.22301 to 341.715326 N, and F from 150 to 425 A·turns. The predefined static stability-region limits resulted in 448 stable and 13,544 unstable samples.

Before training the machine learning models, the computational database was divided into training and testing subsets. The training subset was used to fit the classification and regression models, while the testing subset was used to evaluate their generalization ability on previously unseen data. In this study, 80% of the data were used for training and 20% was used for testing. The same train–test splitting strategy was applied to both classification and regression tasks to ensure a consistent comparison of the considered algorithms.

The general structure of the database is as follows. The first column contains the air gap g, the second column contains the magnetomotive force F, and the third column contains the electromagnetic attractive force P_E. Therefore, each operating point can be represented as:

$$X_i = \left(g_i, F_i, P_{E,i}\right) \quad (6)$$

where: i is the index of the calculated operating point.

For the classification task, each operating point was labeled according to the stability-region conditions. If the values of g_i and $P_{E,i}$ satisfied the predefined allowable limits, the point was assigned to the stable class. Otherwise, it was assigned to the unstable class. Thus, the labeled dataset for classification can be written as:

$$D_c = \{(X_i, y_i)\}_{i=1}^{N} \quad (7)$$

where: N is the total number of operating points in the database, X_i is the input vector, and $y_i \in \{0,1\}$ is the corresponding class label.

The classification problem was solved using three supervised learning algorithms: Random

Forest Classifier, Gradient Boosting Classifier, and Decision Tree Classifier [28]. These algorithms were selected because they are suitable for tabular engineering datasets, can model nonlinear relationships between variables, and provide efficient classification performance without requiring explicit analytical expressions for the decision. The main objective of the classification stage was to determine whether a given operating point belongs to the predefined stability region.

The performance of the classification algorithms was evaluated using the area under the receiver operating characteristic curve (AUC), which was used as the main classification quality metric. Since the classification dataset was imbalanced, additional threshold-dependent metrics were also calculated, including accuracy, precision, recall, F1-score, and balanced accuracy. These metrics were used to provide a more complete evaluation of the ability of the classifiers to identify stable and unstable operating points. In addition, the confusion matrix and receiver operating characteristic (ROC) curve were analyzed for the best-performing classifier to evaluate the distribution of correctly and incorrectly classified operating points.

For the prediction task, a regression formulation was used. In this case, the purpose was to predict the required magnetomotive force for specified values of the air gap and electromagnetic attractive force. Therefore, the input vector for the regression model was defined as

$$Z_i = \left(g_i, P_{E,i}\right) \tag{8}$$

while the target variable was the magnetomotive force F_i. The regression dataset can be expressed as:

$$D_r = \{(Z_i, F_i)\}_{i=1}^{N} \tag{9}$$

Four regression algorithms were trained and compared: Random Forest Regressor, Gradient Boosting Regressor, MLP Regressor [28], and CatBoost Regressor [29]. These models were selected to compare ensemble tree-based methods, neural-network-based prediction, and gradient boosting approaches. The prediction performance was evaluated using the coefficient of determination (R^2), mean squared error (MSE), root mean square error (RMSE), mean absolute error (MAE), mean absolute percentage error (MAPE), maximum absolute error, and percentage error. In addition, training time and prediction time were recorded for each algorithm to evaluate computational efficiency. The coefficient of determination is defined as:

$$R^2 = 1 - \frac{\sum_{i=1}^{N}\left(F_i - \hat{F}_i\right)^2}{\sum_{i=1}^{N}\left(F_i - \bar{F}\right)^2} \tag{10}$$

where: F_i is the actual magnetomotive force, $\hat{F}_i$ is the predicted magnetomotive force, and $\bar{F}$ is the mean value of the actual magnetomotive force.

The complete workflow of the proposed methodology consists of the following stages. First, the mathematical model of the lifting electromagnet is used to generate the computational database. Second, the stability region is defined according to the allowable ranges of the air gap and electromagnetic attractive force. Third, the database is labeled for binary classification based on the stability-region conditions. Fourth, classification algorithms are trained to identify stable and unstable operating points. Fifth, regression algorithms are trained to predict the required magnetomotive force for specified values of g and P_E. Finally, the predicted magnetomotive force values are analyzed from the viewpoint of electromagnetic performance and control coil thermal feasibility.

This methodology enables the transformation of a computationally intensive design procedure into a machine learning-assisted framework. The classification stage provides a rapid assessment of whether the considered electromagnet can operate within the predefined stability region, while the regression stage provides the magnetomotive force values required for maintaining the load in suspension mode.

CLASSIFICATION RESULTS AND STATIC STABILITY ASSESSMENT

The aim of the machine learning-assisted classification of the calculated operating points of the lifting electromagnet was to determine whether each operating point belongs to the predefined stability region. According to the formulation, an operating point was assigned to the stable class if the corresponding air gap and electromagnetic attractive force satisfied the predefined limits. Otherwise, the point was assigned to the unstable class.

The classification models were trained and tested using the computational database. The input variables for the classification task were the air gap g and electromagnetic attractive force P_E. The output variable, as stated above, was the binary class label y, where y = 1 denotes an operating point inside the stability region and y = 0 denotes an operating point outside this region.

Three classification algorithms were compared: Random Forest Classifier, Gradient Boosting Classifier, and Decision Tree Classifier. The obtained results are summarized in Table 2.

As shown in Table 2, the classification dataset was imbalanced, containing 13,544 samples of class (y=0) and 448 samples of class (y=1). Therefore, accuracy alone is not sufficient for evaluating the classification performance, and additional threshold-dependent metrics, including precision, recall, F1-score, and balanced accuracy, were also analyzed.

All three classifiers demonstrated high performance on the considered dataset. The Random Forest Classifier achieved an AUC value of 0.999 and an accuracy of 0.9987. Its precision was equal to 1.000, while the recall was 0.9598, indicating that the model did not produce false positive predictions for the stable class but missed a small number of stable operating points. The Gradient Boosting Classifier also showed high classification quality, with an AUC value of 0.990, accuracy of 0.9997, precision of 0.9978, recall of 0.9933, F1-score of 0.9955, and balanced accuracy of 0.9933.

The best result was obtained using the Decision Tree Classifier, which achieved an AUC value of 1000 and perfect values of accuracy, precision, recall, F1-score, and balanced accuracy. This result indicates that, for the deterministic static stability-region labeling rule used in this study, the Decision Tree Classifier reproduced the predefined admissible-region boundary without classification errors. The feature-importance values also confirm that the class label is mainly determined by the electromagnetic attractive force P_E and the air gap g. For the Decision Tree Classifier, the feature importance values were 0.513 for P_E and 0.487 for g, which is consistent with the definition of the static stability region in the (g, P_E) plane.

To further verify the robustness of the classification result, 10-fold cross-validation was performed for the Decision Tree Classifier. The obtained metrics were stable across all folds, with AUC = 1.0000 ± 0.0000, accuracy = 1.0000 ± 0.0000, balanced accuracy = 1.0000 ± 0.0000, and F1-score = 1.0000 ± 0.0000. These results confirm that, for the generated dataset and the deterministic static stability-region labeling rule, the Decision Tree Classifier consistently reproduced the predefined admissible-region boundary.

The prediction time of all classifiers was very small, varying from 1×10^{-7} s to 7×10^{-7} s per operating point. Among the considered algorithms, the Decision Tree Classifier provided both the highest classification accuracy and the shortest training and prediction times. Therefore, it was selected as the most suitable classifier for rapid design-stage identification of operating points belonging to the predefined static stability region.

The confusion matrix obtained for the Decision Tree Classifier confirmed that all testing points were correctly classified (Figure 3a). This result indicates that, for the considered stability-region definition and generated computational database, the Decision Tree Classifier was able to identify the boundary between admissible and inadmissible operating states without classification errors. The corresponding ROC curve also confirmed perfect class separability, since the AUC value was equal to 1.000 (Figure 3b).

Table 2. Performance comparison of classification algorithms on the dataset

Classification algorithm	AUC	Accuracy	Precision	Recall	F1-score	Balanced accuracy	Class distribution	Feature importance	Training time, s	Pred. time,s
Random Forest Classifier	0.999	0.9987	1	0.9598	0.9795	0.9799	y=0: 13544, y=1: 448	P_E: 0.640807 g: 0.359193	3	1×10^{-7}
Gradient Boosting Classifier	0.990	0.9997	0.9978	0.9933	0.9955	0.9933	y=0: 13544, y=1: 448	P_E: 0.619395 g: 0.380605	2	3×10^{-7}
Decision Tree Classifier	1.000	1.000	1.000	1.000	1.000	1.000	y=0: 13544, y=1: 448	P_E: 0.513 g: 0.487	1	1×10^{-7}

From an engineering viewpoint, the classification results show whether the investigated lifting electromagnet configuration can provide the required operating states within the predefined stability region. Points classified as stable correspond to combinations of g and P_E for which the electromagnet satisfies the suspension condition. Points classified as unstable correspond to operating states where either the air gap or the electromagnetic attractive force lies outside the allowable limits.

The classification results obtained using the Decision Tree Classifier are shown in Figure 4. In this figure, the operating points belonging to the stability region are marked separately from the points located outside the admissible region. The obtained distribution confirms that the considered electromagnet design provides the necessary combinations of air gap, electromagnetic attractive force, and magnetomotive force within the specified stability region. Therefore, the investigated design variant can be considered suitable for maintaining the load in suspension mode under the adopted stability constraints.

It should be noted that the classification model does not replace the physical mathematical model of the electromagnet. Instead, it serves as a data-driven tool for rapid assessment of calculated operating points. Once trained, the classifier can quickly determine whether an operating point satisfies the stability requirements, thereby reducing the need for repeated direct evaluation of the mathematical model during preliminary design analysis.

This classification stage provides the first part of the proposed stability assessment framework. However, identifying stable operating points is not sufficient for complete design verification. It is also necessary to determine the magnetomotive force required to realize the desired air gap and electromagnetic attractive force. For this reason, the next stage of the study focuses on regression-based prediction of the required magnetomotive force.

PREDICTION OF THE REQUIRED MAGNETOMOTIVE FORCE

Based on the training and testing results of the considered regression algorithms, the CatBoost Regressor demonstrated the best prediction performance for determining the required magnetomotive force during the design stage of the lifting electromagnet. This model achieved the highest coefficient of determination among the considered regression algorithms and provided a more accurate prediction of F for different combinations of the air gap g and electromagnetic attractive force P_E. The obtained results are summarized in Table 3.

Table 3 presents the testing performance and computational efficiency of the considered regression algorithms. The Random Forest Regressor achieved an R^2 value of 0.9276, with RMSE = 21.6866 A·turns, MAE = 12.1498 A·turns, and MAPE = 4.6155%. The Gradient Boosting Regressor provided significantly better accuracy, with (R^2 = 0.9986), RMSE = 2.9232 A·turns,

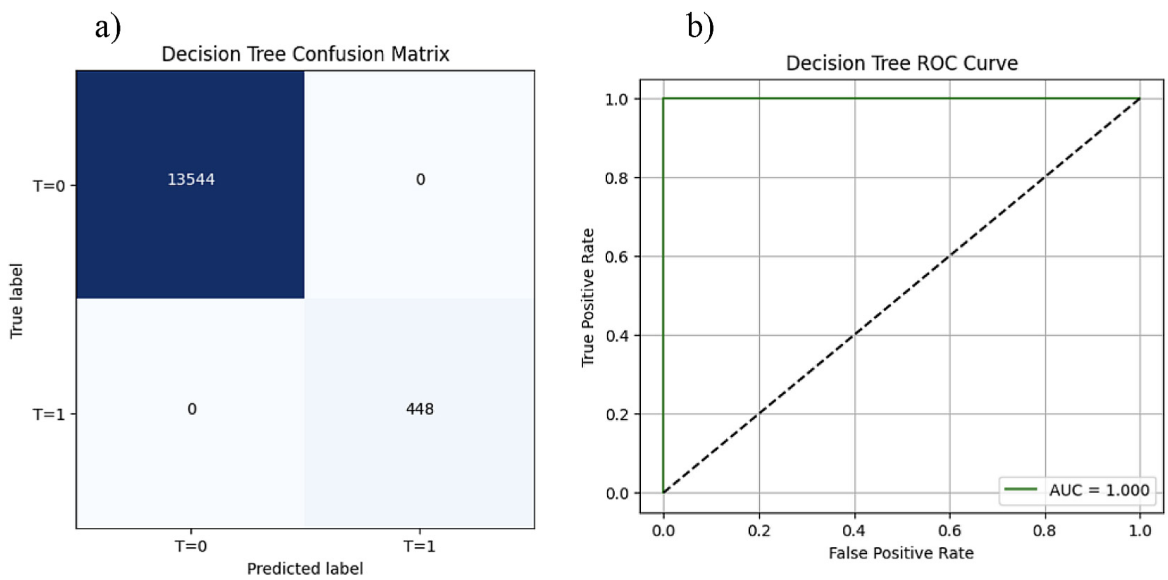

Figure 3. Confusion matrix (a) and ROC curve (b) for the Decision Tree Classifier

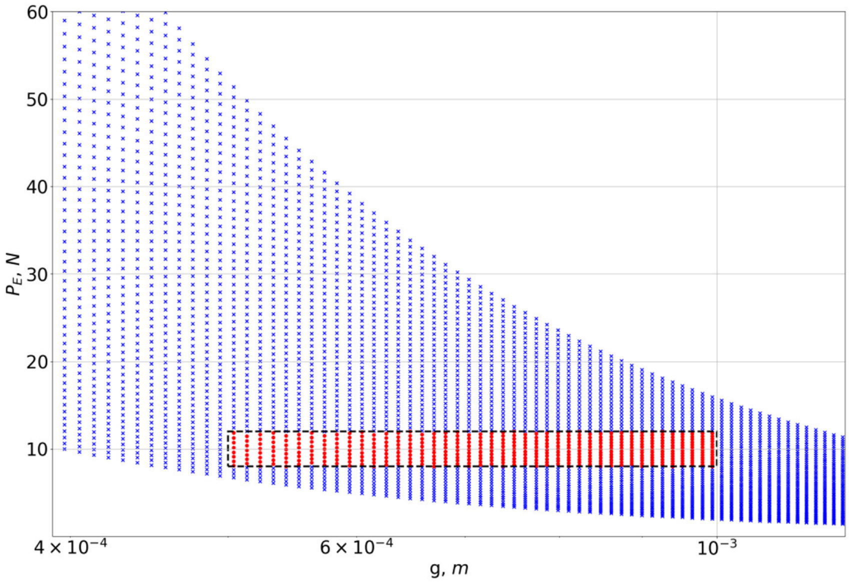

Figure 4. Classification results obtained using the Decision Tree Classifier

MAE = 2.2464 A·turns, and MAPE = 0.835%. The MLP Regressor also achieved high prediction accuracy, with $R^2 = 0.9887$, but required the longest training time of 144 s.

Among the considered models, the CatBoost Regressor achieved the best overall prediction accuracy according to the averaged error metrics, with $R^2 = 0.9995$, MSE = 3.216, RMSE = 1.7933 A·turns, MAE = 1.2747 A·turns, and MAPE = 0.4631%. Although the Gradient Boosting Regressor showed a slightly lower maximum absolute error than CatBoost, the CatBoost Regressor provided the best overall performance according to R^2, MSE, RMSE, MAE, and MAPE. For the CatBoost Regressor, ehe maximum absolute error was 12.8563 A·turns, while the maximum percentage error was 7.9783%. The total prediction time was 0.0642 s for the testing dataset, corresponding to approximately 0.000023 s per sample on the online computational platform used in this study. The 95% confidence interval for MAE was [1.2279, 1.3214] A·turns, indicating a narrow uncertainty range for the average absolute prediction error.

For comparison, on the same computational platform, the average calculation time of the original mathematical model for a single inverse-problem evaluation was 0.5681 s [27]. Therefore, the trained CatBoost surrogate provides an acceleration factor of approximately 24,700 for repeated design-stage magnetomotive-force prediction within the considered operating range. This result indicates that the trained regression model can be used as an efficient surrogate tool for rapid estimation of the required magnetomotive force without repeatedly solving the original mathematical model.

To further evaluate the robustness of the best regression model, 10-fold cross-validation was performed for the CatBoost Regressor. The obtained average cross-validation results were $R^2 = 0.9994 \pm 0.0001$, RMSE = 1.8956 ±

Table 3. Performance comparison of regression algorithms on the testing dataset

Regression algorithm	R^2	MSE	RMSE, A·turns	MAE, A·turns	MAPE, %	Max absolute error, A·turns	Training time, s	Prediction time, s
Random Forest Regressor	0.9276	470.3087	21.6866	12.1498	4.6155	110	7	0.000012
Gradient Boosting Regressor	0.9986	8.5451	2.9232	2.2464	0.8350	11.2348	6	0.000011
MLP Regressor	0.9887	73.2717	8.5598	5.7320	2.2335	58.2846	144	0.00002
CatBoost Regressor	0.9995	3.2160	1.7933	1.2747	0.4631	12.8563	54	0.000023

0.1644, MAE = 1.3094 ± 0.0569, and MAPE = 0.4765% ± 0.0242%. The small standard deviations of these metrics indicate that the CatBoost Regressor maintained stable prediction accuracy across different data folds.

The characteristic prediction results obtained using the CatBoost Regressor are presented in Figure 5. As shown in Figure 5a, the predicted values are located almost entirely along the 45-degree reference line, indicating good agreement between the reference values obtained from the mathematical model and the predicted values. The deviations between the reference and predicted values are small over the entire considered range of F, although a small number of points show slightly larger deviations at the lower part of the F range. Figure 5b shows that most residuals are concentrated within approximately ±5% A·turns, while the maximum absolute residual is 12.8563 A·turns. These results are consistent with the error metrics reported in Table 3 and confirm the high prediction accuracy of the CatBoost Regressor for the considered dataset.

For the characteristic points of the stability region, namely the boundary points 1, 1', 2, 2', and the central point 0, the corresponding values of the magnetomotive force were predicted using the trained CatBoost Regressor model. The obtained results are presented in Table 4.

Table 4 compares the magnetomotive force values predicted by the CatBoost Regressor with the reference values obtained from the mathematical model for the characteristic points of the predefined static stability region. The obtained errors are small for all considered points. The absolute error varies from 0.037838 A·turns to 0.714910 A·turns, while the percentage error does not exceed 0.2377%. The mean absolute error for these characteristic points is 0.3214 A·turns, and the corresponding mean absolute percentage error is 0.1262%.

The data presented in Table 4 show that the maximum value of the magnetomotive force is obtained at point 2, where g = 0.001 *m* and P_E = 12 N. The minimum value is obtained at point 1’, where g = 0.0005 *m* and P_E = 8 *N*. The central point 0, with values g = 0.00075 *m* and P_E = 10 *N*, corresponds to an intermediate value of the required magnetomotive force.

The predicted characteristic values of the magnetomotive force are important for evaluating the operational feasibility of the designed electromagnet. In particular, the predicted *F* values can be used to assess whether the temperature rise of the control coil remains within the allowable thermal limit of the winding conductor. If the control coil temperature corresponding to the predicted magnetomotive force exceeds the permissible value, the electromagnet design must be revised.

The predicted dependencies of the magnetomotive force on the electromagnetic attractive force for different values of the air gap are shown in Figure 6. The curves were obtained for g = 0.0005, 0.000625, 0.00075, 0.000875, and 0.001 *m*. In addition, Figure 7 presents the predicted dependencies of the magnetomotive force on the air gap for different values of the electromagnetic attractive force, namely P_E = 8, 9, 10, 11 and 12 *N*.

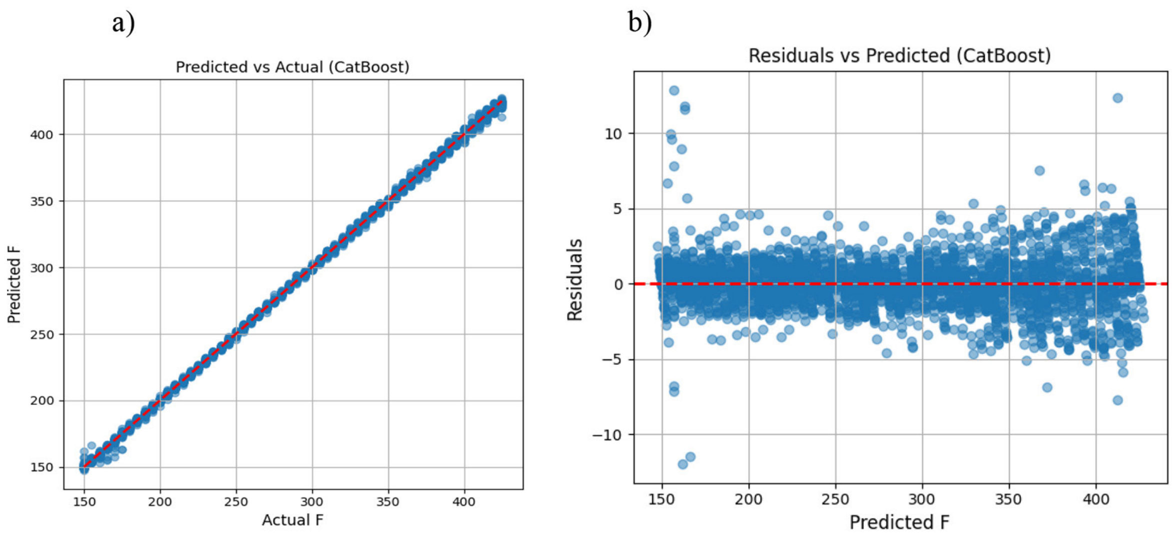

Figure 5. Characteristic prediction results of the CatBoost Regressor: (a) relationship between predicted and actual values; (b) residuals as a function of predicted values

The obtained dependencies are physically consistent with the operating principles of a lifting electromagnet. For a fixed air gap, an increase in the electromagnetic attractive force leads to an increase in the required magnetomotive force. Similarly, for a fixed electromagnetic attractive force, an increase in the air gap requires a higher magnetomotive force because the magnetic reluctance of the air gap increases. Therefore, the predicted curves confirm that the trained CatBoost Regressor model preserves the expected physical behavior

Table 4. Comparison of predicted and mathematical-model values of the magnetomotive force for characteristic points of the static stability region

Static stability region point	g, m	P_E , N	Predicted F, A·turns	Mathematical model F_{model}, A·turns	Absolute error, A·turns	Percentage error, %
1	0.0005	12	201.853589	201.75	0.103589	0.0513
1′	0.0005	8	163.199278	163.01	0.189278	0.1161
0	0.00075	10	259.468781	260.03	0.561219	0.2158
2	0.001	12	370.287838	370.25	0.037838	0.0102
2′	0.001	8	300.035090	300.75	0.714910	0.2377

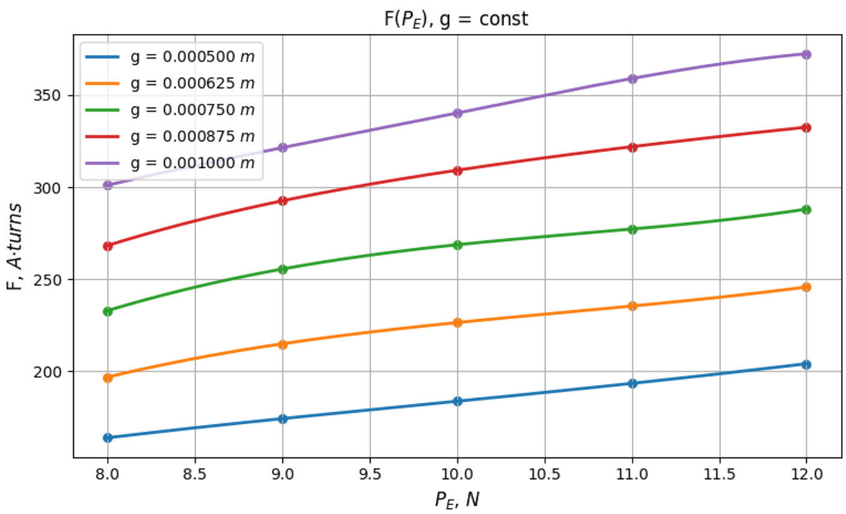

Figure 6. Predicted magnetomotive force as a function of electromagnetic attractive force for different air-gap values

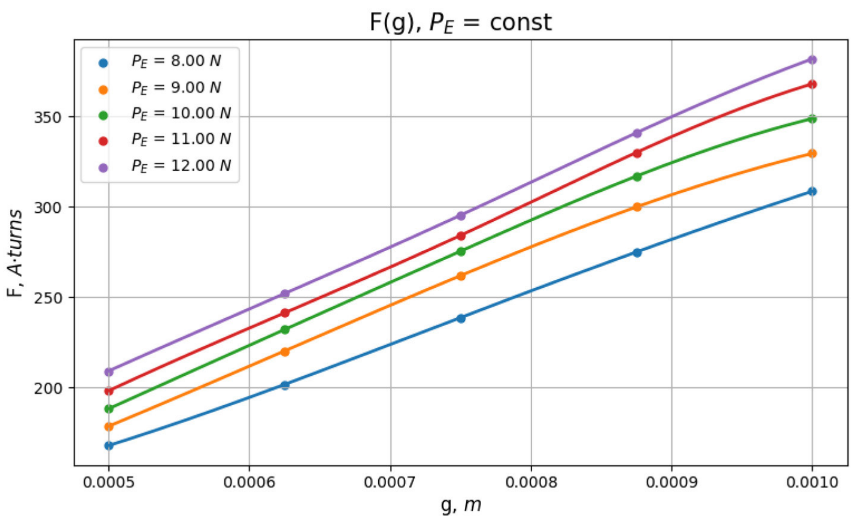

Figure 7. Predicted magnetomotive force as a function of air gap for different electromagnetic attractive force values

of the lifting electromagnet within the considered stability region.

In summary, the regression-based prediction stage demonstrated that the required magnetomotive force can be accurately estimated from the air gap and electromagnetic attractive force using the trained CatBoost Regressor model. The obtained R^2 value, short prediction time, and physically consistent dependencies confirm the suitability of the proposed model for rapid design-stage calculations. The predicted magnetomotive force values for characteristic points of the stability region provide important information for further verification of the control coil thermal feasibility. Thus, the regression model complements the classification stage by not only identifying admissible operating states, but also determining the control action required to maintain the load in suspension mode.

The obtained results should be interpreted within the scope of the proposed static design-stage formulation. The present study demonstrates classification of operating points with respect to a predefined static stability region and regression-based prediction of the magnetomotive force for a model-generated dataset. It does not demonstrate dynamic suspension stability, real-time feedback control performance, disturbance rejection, or full thermal feasibility of the control coil. The predicted magnetomotive force values should therefore be regarded as input information for subsequent thermal verification rather than as direct evidence of thermal feasibility. In a preliminary design workflow, the trained classifier can be used to rapidly identify whether a candidate operating point belongs to the admissible static operating region, while the trained regression model can estimate the magnetomotive force required for specified values of the air gap and electromagnetic attractive force. Since the database was generated for a fixed electromagnet geometry, material properties, and operating ranges, application to other geometries or extended ranges would require database regeneration or extension and retraining of the machine learning models.

CONCLUSIONS

This study proposed a machine learning-assisted framework for design-stage evaluation of a lifting electromagnet operating in suspension mode, combining static stability-region classification with magnetomotive force prediction. A computational database was generated from the mathematical model of the electromagnet and used to formulate two related tasks: binary classification of operating points with respect to a predefined static stability region and regression-based prediction of the required magnetomotive force.

The classification results showed that all considered algorithms provided high performance, with the Decision Tree Classifier achieving the best result for the considered dataset, reaching an AUC value of 1.000 with a training time of 1 s. This confirms that the proposed classification formulation can effectively distinguish admissible and inadmissible operating states within the specified air-gap and electromagnetic-force limits. However, this result should be interpreted within the scope of the deterministic static stability-region labeling rule and should not be considered as verification of dynamic suspension stability.

For magnetomotive force prediction, the CatBoost Regressor achieved the best overall performance among the evaluated regression models, with R^2=0.9995, RMSE = 1.7933 A·turns, MAE = 1.2746 A·turns, and MAPE = 0.4630%. These results confirm that the trained regression model can accurately approximate the deterministic relationship between the air gap, electromagnetic attractive force, and required magnetomotive force within the considered operating range.

The predicted values for the characteristic points of the static stability region were physically consistent: the required magnetomotive force increased with both the air gap and the electromagnetic attractive force. At these points, the predicted magnetomotive force values were compared with the reference values obtained from the mathematical model. The maximum absolute error was 0.7149 A·turns, and the maximum percentage error did not exceed 0.2377%, indicating that the trained CatBoost Regressor accurately reproduced the mathematical-model results at the boundary and central points of the considered region.

The obtained results show that the proposed approach can serve as an efficient data-driven tool for preliminary design-stage analysis. The classification model enables rapid static operating-region assessment, while the regression model provides the magnetomotive force values required for suspension operation and subsequent evaluation of the control coil thermal feasibility.

Future work will focus on extending the proposed framework to different electromagnet geometries and operating conditions, experimental validation of the predicted values, integration into automated design software, and consideration of multi-objective criteria such as electromagnetic performance, power consumption, material cost, and thermal constraints. In addition, dynamic behavior, feedback control performance, disturbance rejection, and full thermal verification should be investigated in future studies to extend the proposed static design-stage framework toward complete suspension-system analysis.

Acknowledgement

This work was supported by the Higher Education and Science Committee of Republic of Armenia, in the frames of the research project №25RG-2B089.

REFERENCES

1. Hashemi A., Gharaei P.Y. A novel method for field analysis and design of electromagnet used in lifting applications. Advanced Electromagnetics, Sep. 2019; 8(4): 32–38, https://doi.org/10.7716/aem.v8i4.1109
2. Hashemi A., Qaraei P.Y. Cylindrical electromagnets: Modeling, analysis, simulation and implementation. COMPEL - The International Journal for Computation and Mathematics in Electrical and Electronic Engineering, 2023; 43(1): 50–65, https://doi.org/10.1108/COMPEL-01-2023-0029
3. Ren W., Wu L., Zhang W., Jiang P., Wang Z., Luo C., Guo J., Liu C., Wei Y., Chen Z. et al. Design and parametric analysis of the constant force characteristics of the electromagnet for hydraulic valves. Processes, 2024; 12(12), Art. no. 2632, https://doi.org/10.3390/pr12122632
4. Liao Y., Liu Y., Xing J., Chen B., Gao L. et al. Electromagnetic force investigation of electromagnets with variable pole area in an electromagnetic diaphragm pump. PLOS ONE, Oct. 2023; 18(10), Art. no. e0292685, https://doi.org/10.1371/journal.pone.0292685
5. Li Y., Lei G., Bramerdorfer G., Peng S., Sun X., Zhu J. Machine learning for design optimization of electromagnetic devices: Recent developments and future directions. Applied Sciences, 2021; 11(4): Art. no. 1627, https://doi.org/10.3390/app11041627
6. Lowther D.A. The application of artificial intelligence and machine learning to the design and analysis of electromagnetic devices. International Journal of Applied Electromagnetics and Mechanics, 2023; 73(4): 565–577, https://doi.org/10.3233/JAE-230104
7. Li Z., Cheng M., Tyrrell A.M., Zhao X. A review of data-driven models for electromagnetic devices design and analysis. IEEE Access, 2025; 13: 142161–142185, https://doi.org/10.1109/ACCESS.2025.3591965
8. Cheng M., Zhao X., Dhimish M., Qiu W., Niu S. A review of data-driven surrogate models for design optimization of electric motors. IEEE Transactions on Transportation Electrification, 2024; 10(4): 8413–8431, https://doi.org/10.1109/TTE.2024.3366417
9. Orosz T., Rassõlkin A., Kallaste A., Arsénio P., Pánek D., Kaska J., Karban P. Robust Design optimization and emerging technologies for electrical machines: Challenges and open problems. Applied Sciences, 2020; 10(19), Art. no. 6653, https://doi.org/10.3390/app10196653
10. Tahkola M., Keränen J., Sedov D., Farzam M. Far, Kortelainen J. Surrogate modeling of electrical machine torque using artificial neural networks. IEEE Access, 2020; 8: 220027–220045, https://doi.org/10.1109/ACCESS.2020.3042834
11. Tucci M., Barmada S., Formisano A., Thomopulos D. A regularized procedure to generate a deep learning model for topology optimization of electromagnetic devices. Electronics, 2021; 10(18), Art. no. 2185, https://doi.org/10.3390/electronics10182185
12. Lei G., Yang G.Y., Shao K.R., Guo Y., Zhu J., Lavers J. D. Electromagnetic device design based on RBF models and two new sequential optimization strategies. IEEE Transactions on Magnetics, Aug. 2010; 46(8): 3181–3184, https://doi.org/10.1109/TMAG.2010.2043717
13. Sarker N., Podder P., Mondal M. R. H., Shafin S.S., Kamruzzaman J. Applications of machine learning and deep learning in antenna design, optimization, and selection: A review. IEEE Access, 2023; 11: 103890–103915, https://doi.org/10.1109/ACCESS.2023.3317371
14. Grigoryan A., Avetisyan A., Harutyunyan L. Optimization of material and operational costs in electromagnet design Eng. Technol. Appl. Sci. Res., Feb. 2026; 16(1): 30971–30977, https://doi.org/10.48084/etasr.13826
15. Grigoryan A, Avetisyan A.G., Melkonyan T, Gulinyan M. Heuristic and machine learning methods for optimizing magnetorheological brake performance. Advances in Science and Technology Research Journal. 2026; 20(4): 317–327. https://doi.org/10.12913/22998624/215203
16. Grigoryan A., Avetisyan A., Chukhajyan N., Hovhannisyan A., Hovsepyan A. Optimal design of an electromagnet using machine learning methods. International Review of Electrical Engineering, 2024; 19(4): 337–345. https://doi.org/10.15866/iree.v19i4.25425

17. Grigoryan A., Avetisyan A., Melkonyan T., Hovhannisyan A., Hovsepyan A. Optimization of parameters of electromagnetic system with magnetorheological fluid. International Review of Electrical Engineering, 2024; 19(5): 410–420. https://doi.org/10.15866/iree.v19i5.25645
18. Grigoryan A., Avetisyan A., Melkonyan T., Yenokyan K. Automated modeling of an electromagnet with magnetorheological fluid. Engineering, Technology & Applied Science Research. Jun. 2025; 15(3): 22937–22944. https://doi.org/10.48084/etasr.10909
19. Zhang Z., Zhou Y., Tao X. Model predictive control of a magnetic levitation system using two-level state feedback. Measurement and Control, 2020; 53(5–6): 962–970, https://doi.org/10.1177/0020294019900333
20. Kim C. Robust air-gap control of superconducting-hybrid maglev intelligent conveyor system in smart factory. IEEE Transactions on Magnetics, Jun. 2019; 55(6), Art. no. 8300705, 1–5, https://doi.org/10.1109/TMAG.2019.2900068
21. Xu J., Chen Y.-H., Guo H. Robust levitation control for maglev systems with guaranteed bounded airgap. ISA Transactions, 2015; 59: 205–214, https://doi.org/10.1016/j.isatra.2015.10.004
22. Xu J., Du Y., Chen Y.-H., Guo H. Adaptive robust constrained state control for non-linear maglev vehicle with guaranteed bounded airgap. IET Control Theory & Applications, 2018; 12(11): 1573–1583, https://doi.org/10.1049/iet-cta.2017.1348
23. Sun Y., Xu J., Wu H., Lin G., Mumtazet S. et al. Deep learning based semi-supervised control for vertical security of maglev vehicle with guaranteed bounded airgap. IEEE Transactions on Intelligent Transportation Systems, 2021; 22(7): 4431–4442, https://doi.org/10.1109/TITS.2020.3045319
24. Feng Y., Zhao C., Liang X., Bai Z. SNN-based surrogate modeling of electromagnetic force and its application in maglev vehicle dynamics simulation. Actuators, 2025; 14(3), Art. no. 112, https://doi.org/10.3390/act14030112
25. Zhou X., Liang S., Li X., Long Z., Wang Z. A data-driven comprehensive evaluation method for electromagnetic suspension maglev control system. Actuators, 2024; 13(8), Art. no. 314, https://doi.org/10.3390/act13080314
26. Liu D., Wu D., Xu J., Li Y., Gul M. Z., Ni F. Machine Learning in Maglev Transportation Systems: Review and Prospects. Actuators, 2025; 14(12), Art. no. 576, https://doi.org/10.3390/act14120576
27. Grigoryan A., Avetisyan A., Hovhannisyan An., Hovhannisyan Ar., Hovsepyan A. A solution method for direct and inverse problems of an electromagnet magnetic circuit. IEEE Access, 2026; 14: 60375–60387, https://doi.org/10.1109/ACCESS.2026.3684728
28. Scikit-learn Documentation. https://scikit-learn.org/stable
29. CatBoost Official Website. https://catboost.ai